

Optimizing EV Charging Behavior: A Data-Driven Analysis of Local and Neighborhood Tariff Impacts

Yimeng Wang
School of Advanced
Technology
Xi'an Jiaotong-Liverpool
University
Suzhou, China

Yimeng.Wang22@student.xjtlu.edu.cn

Lurui Fang *
School of Advanced
Technology
Xi'an Jiaotong-Liverpool
University
Suzhou, China

Lurui.Fang@xjtlu.edu.cn
*Corresponding author

Yanxi Lyu
School of Advanced
Technology
Xi'an Jiaotong-Liverpool
University
Suzhou, China

Yanxi.Lyu18@student.xjtlu.edu.cn

Xiaoyang Chen
School of Advanced
Technology
Xi'an Jiaotong-Liverpool
University
Suzhou, China

Xiaoyang.Chen02@xjtlu.edu.cn

Saqib Khurshed
School of Electrical
Engineering, Electronics and
Computer Science
University of Liverpool
Liverpool, UK

S.Khurshed@liverpool.ac.uk

Eng Gee Lim
School of Advanced
Technology
Xi'an Jiaotong-Liverpool
University
Suzhou, China
enggee.lim@xjtlu.edu.cn

Abstract—This paper proposes a data-driven methodology to analyze the impact of local and neighborhood tariffs on electric vehicle (EV) charging behavior. The study uses real-world data from public charging piles. It uses LSTM based dimensionality reduction, K-Means clustering based on cosine similarity and decision tree regression. It divides the charging stations into different clusters based on pricing model and occupancy. The results show that: (1) Occupancy rates show marked improvement when implementing dynamic pricing with competitively positioned local tariffs; (2) Rigid high-tariff frameworks persistently diminish utilization regardless of external pricing conditions; (3) The most deficient performance emerges in balanced tariff configurations (where local rates are marginally below adjacent stations yet both maintain static pricing). The proposed methodology is practical, offering actionable insights for optimizing pricing strategies and enhancing the efficiency of urban EV charging networks.

Keywords—electric vehicle (EV) charging behavior, dynamic pricing strategies, local and neighborhood tariffs

I. INTRODUCTION

The electric vehicle can reduce greenhouse gas emissions and environmental pollution compared with traditional fuel vehicles. Therefore, it has been vigorously promoted by governments around the world. According to the latest industry report released by Gartner, including cars, buses, vans and heavy trucks, global electric vehicle ownership will reach 64 million units in 2024, and is expected to grow 33% year-on-year to 85 million units in 2025 [1]. With the rapid growth in the number of electric vehicles, recent studies indicate that infrastructure design and subsidy policies critically influence charging station profitability and utilization patterns [2,3], while the demand for

electric vehicle charging is also on the rise, placing higher demands on the charging infrastructure's ability to guarantee services.

Recognizing the unsustainability of ever-expanding EV charging space, recent studies advocate the application of smart pricing strategies (e.g., dynamic pricing and co-pricing) to optimize urban EV charging [4]. A critical prerequisite for such optimization is understanding how EV charging behavior adjusts to fluctuations in electricity prices. There is increasing recognition that this line of research is critical to advancing vehicle electrification and rethinking sustainable transportation [5].

In numerous studies, pricing has been identified as a critical factor influencing users' decisions when selecting a charging station [6]. This sensitivity to price exhibits spatial variability, with urban users displaying higher elasticity owing to the presence of alternative transportation choices [7]. Regression models are typically used to quantify pricing effects. These models can analyze relationships between variables, generate impulse responses, and estimate the price elasticity of demand (measuring how demand responds to price changes) [8]. In recent years, machine learning approaches like XGBoost have proven effective in capturing nonlinear charging behavior patterns while identifying critical features such as charging speed and station availability [9]. Such studies have proposed the use of machine learning techniques to model nonlinear relationships between variables [10]. Such studies provide concepts for regional demand-side management for smart charging of electric vehicles. However, they focus mainly on the local situation and ignore the corresponding price changes in the neighboring regions.

Advancements in data collection and storage technologies have enabled the widespread adoption of data-driven approaches and neural networks to model the intricate relationships between electric vehicle charging demand and pricing dynamics [11]. Additionally, policy-driven measures such as time-of-use tariffs and infrastructure subsidies further influence these interactions [12,13]. Despite these developments, there remains a gap in leveraging data-driven methods and neural networks to investigate how local electricity price characteristics impact charging pile occupancy rates.

Based on the literature review, there is a gap in linking neighborhood electricity pricing with user charging behavior. Most studies focus on the direct impact of charging prices. They use machine learning to model nonlinear relationships, while ignoring the impact of prices in the surrounding area on user decisions.

This paper presents an approach that combines neighborhood tariffs and charging behavior analysis. It uses original data from charging stations to categorize user behavior. Then, it examines the behavior of different categories of users in response to their own rates and nearby rates. It provides insights to improve pricing and operational efficiency. First, the data are labeled to distinguish different charging states and to calculate key metrics such as charging station prices, neighborhood tariffs and their differences. Then, the data are normalized to ensure the consistency of the variables. Next, based on the existing charging behavior framework [8], selected clustering method, sampling the K-means clustering method. Charging stations are grouped based on price and usage patterns. Finally, the clustering results reveal the relationship between local and neighborhood electricity prices and user charging behavior. This paper has the following practical contributions:

1. This study develops a comprehensive framework that integrates neighborhood tariffs and user behavior analysis, enabling the classification of charging stations into distinct clusters based on pricing patterns and occupancy rates.
2. By analyzing the response behavior of users to local and neighboring tariffs, this paper provides actionable insights for optimizing pricing strategies. For example, when local tariffs are lower than those in neighboring regions, a dynamic pricing strategy greatly increases occupancy, while a fixed high tariff strategy tends to discourage demand.
3. The proposed methodology leverages classic algorithms with low tuning difficulties, such as LSTM-based dimensionality reduction, cosine similarity-based K-means clustering, and decision tree regression. This ensures simplicity in application.

II. METHODOLOGY

The data-driven approach to analyzing charging behavior and user characteristics consists of three phases. In the first phase, original data is organized and scaled. Variance metrics are computed to capture pricing bias. In the second phase, an LSTM network extracts temporal dynamics and reduces data dimensionality. In the third phase, cluster the data and use regression to determine the clustering results and select the clustering method with the best performance. Then, the results

are reflected back to the original data for detailed analysis of charging behavior and user characteristics. The flowchart of the developed method is shown below.

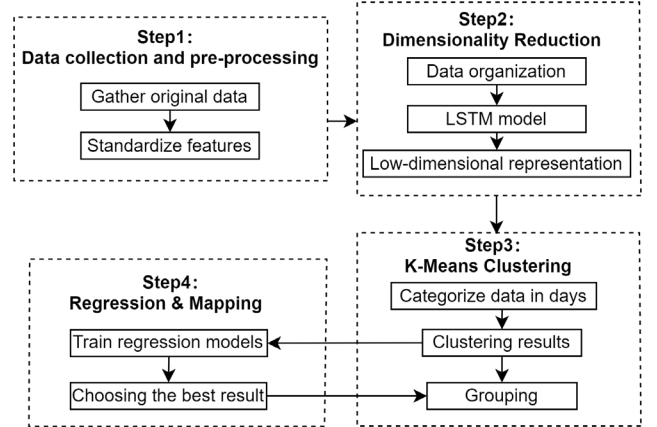


Fig.1. Data-Driven Analysis Approach

A. Data Preprocessing

The charging station data undergoes cleaning and preprocessing. The dataset contains timestamps, neighborhood price, station price, Central Business District (CBD) flag, dynamic pricing flag, count of neighboring stations, and the CBD/dynamic pricing status of neighboring stations. From these data, we derive variance metrics to quantify pricing deviations:

$$diff = P_{station} - P_{neigh} \quad (1)$$

In these equations, $P_{station}$ is the station price, P_{neigh} is the maximum neighborhood price.

Normalization is performed to eliminate scale differences. Scale features to their maximum value, the features include: timestamps, CBD flag, dynamic pricing flag, count of neighboring stations, CBD/dynamic pricing status of neighboring stations.

$$F_s = \left\{ \frac{c_1}{c_{1,max}}, \frac{c_2}{c_{2,max}}, \dots, \frac{c_n}{c_{n,max}} \right\} \quad (2)$$

Here, c_1 represents the i_{th} feature, and $c_{1,max}$ is its maximum value. This normalization facilitates uniform treatment of variables in subsequent analysis and improves the performance of time-series and clustering models. The demand data is organized into a matrix D_{yp} :

$$D_{yp} = \begin{bmatrix} d_{p,1,1} & \dots & d_{p,1,n_{dt}} \\ \vdots & \ddots & \vdots \\ d_{p,d,1} & \dots & d_{p,d,n_{dt}} \end{bmatrix} \quad (3)$$

where $d_{p,d,n_{dt}}$ give the demand data at the n_{dt}^{th} time interval of the d^{th} day (with $d=21$ days in this paper); n_{dt} is the total number of sampling points throughout a day, and $n_{dt} = 144$ is adopted in this paper. In other words, the data sampling time interval is 10 minutes each day. The dataset includes data from 247 charging stations.

B. LSTM-Based Dimensionality Reduction

The standardized features are organized into a three-dimensional tensor:

$$X \in \mathbb{R}^{N \times T \times D} \quad (4)$$

where N is the number of charging stations, T is the number of time steps per station, and D is the number of features. An LSTM [4] network with 64 hidden units (using ReLU activation) processes the input tensor X to compute hidden states:

1. Forget Gate

$$f_t = \sigma(W_f \cdot [H_{t-1}, X_t] + b_f) \quad (5)$$

where f_t is the forget gate output, computed using the sigmoid activation function σ . W_f is the weight matrix, H_{t-1} is the previous hidden state, X_t is the current input, and b_f is the bias term. The forget gate f_t decides how much of the previous cell state C_{t-1} to forget.

2. Input Gate

$$i_t = \sigma(W_i \cdot [H_{t-1}, X_t] + b_i) \quad (6)$$

where i_t is the input gate output, computed using the sigmoid activation function σ . W_i is the weight matrix, and b_i is the bias term.

The input gate i_t controls how much of the new candidate cell state \bar{C}_t to add.

3. Candidate Cell State

$$\bar{C}_t = \tanh(W_C \cdot [H_{t-1}, X_t] + b_C) \quad (7)$$

where \bar{C}_t is the candidate cell state, computed using the tanh activation function. W_C is the weight matrix, and b_C is the bias term. The candidate cell state represents new information that could be added to the cell state.

4. Cell State Update

$$C_t = f_t \cdot C_{t-1} + i_t \cdot \bar{C}_t \quad (8)$$

where C_t is the updated cell state, combining the previous cell state C_{t-1} and the candidate cell state \bar{C}_t . The cell state C_t is updated by combining retained and new information.

5. Output Gate

$$o_t = \sigma(W_o \cdot [H_{t-1}, X_t] + b_o) \quad (9)$$

where o_t is the output gate output, computed using the sigmoid activation function σ . W_o is the weight matrix, and b_o is the bias term. The output gate o_t determines how much of C_t to output as the hidden state.

6. Hidden State

$$H_t = o_t \cdot \tanh(C_t) \quad (10)$$

where H_t is the hidden state at the current time step, computed by applying the output gate to the updated cell state. The hidden state is passed to the next time step and used for predictions.

The resulting hidden states $H \in \mathbb{R}^{N \times T \times 64}$ are projected into a low-dimensional space using a dense layer:

$$F_t = W_d \cdot H_t + b_d \quad (11)$$

where F_t is the reduced-dimensional output, W_d is the weight matrix, and b_d is the bias term. The final output $F \in \mathbb{R}^{N \times T \times 64}$ preserves essential time-dependent features while reducing redundancy, enhancing computational efficiency for clustering.

C. K-means Clustering Based on Cosine Similarity

The low-dimensional representation F serves as input for clustering. A K-means clustering method based on cosine similarity is used to group charging stations exhibiting similar temporal and pricing patterns.

Cosine similarity between two feature vectors f_i and f_j is defined as:

$$\text{cosine}_{\text{sim}(f_i, f_j)} = \frac{f_i \cdot f_j}{\|f_i\| \|f_j\|} \quad (12)$$

This similarity is transformed into a distance metric:

$$d_{\text{cosine}}(f_i, f_j) = 1 - \text{cosine}_{\text{sim}(f_i, f_j)} \quad (13)$$

The clustering objective minimizes the sum of cosine distances between samples and their corresponding centroids:

$$J = \sum_{i=1}^K \sum_{f \in C_i} \left(1 - \frac{f \cdot \mu_i}{\|f\| \|\mu_i\|} \right) \quad (14)$$

Here, K represents the number of clusters, C_i the set of samples in cluster i , and μ_i the centroid of that cluster. Normalization to unit length prior to clustering ensures the distance reflects only directional differences. This method distinguishes groups with similar charging behavior and pricing patterns.

Simultaneously, the demand data D_{yp} (defined in Equation 3) is directly subjected to K-means clustering. Let the number of clusters be n_{cl} ; the clustering results are denoted by:

$$C_d = \{D_{yp,1}, D_{yp,2}, \dots, D_{yp,n_{cl}}\} \quad (15)$$

Each cluster D_{yp,n_c} corresponds to a set of demand samples, whose demand curve serves as the typical demand profile.

D. Decision Tree Regression Fitting and Mapping Analysis

After clustering, regression models predict the occupancy rate y for each station based on original features. The objective is to minimize the mean squared error (MSE):

$$\min_g \frac{1}{N} \sum_{i=1}^N (y_i - g(x_i))^2 \quad (16)$$

Here, x_i is the feature vector for station i . A decision tree model splits data by minimizing MSE::

$$\text{MSE} = \frac{1}{|S|} \sum_{x_i \in S} (y_i - \bar{y})^2 \quad (17)$$

Additional regression techniques, including Gradient Boosting, Random Forest, LightGBM, MLP, AdaBoost, and CatBoost, also contribute to performance comparisons. The

model performance is evaluated using root mean squared error (RMSE):

$$RMSE = \sqrt{\frac{1}{N} \sum_{i=1}^N (y_i - \hat{y}_i)^2} \quad (18)$$

Predicted occupancy rates are mapped back to the original dataset. This mapping facilitates a detailed analysis of charging behavior and user characteristics across clusters.

III. CASE STUDY

This section presents the numerical results: 1) Section A describes the data description and site locations; 2) Section B gives the selection of clustering methods and the clustering results; 3) Section C characterizes the different clusters, respectively; and 4) Section D discusses the results. In addition, a comparative analysis with other algorithms demonstrates the superiority of the algorithm applied in this study.

A. Data preprocessing and feature selection

The ST-EVCDP dataset used in this study is sourced from a publicly accessible mobile application that monitors the real-time occupancy status of charging piles (idle/occupied)[14]. The dataset covers 18,061 public charging piles across Shenzhen, China, with 5-minute resolution data spanning 30 consecutive days (19 June - 18 July 2022). The urban spatial structure is represented as graph data visualized in Figure 2.

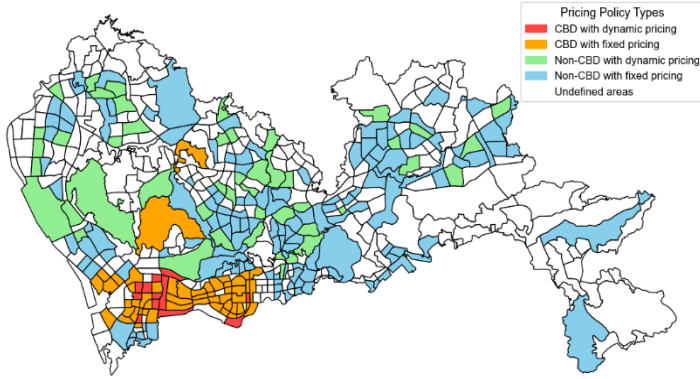


Fig. 2. Distribution of Public EV Charging Pile Distribution in Shenzhen

TABLE I. DESCRIPTIVE STATISTICS OF EV CHARGING DATASET.

Region*	P_average*	Occ_rate*	N_neig*	Dyn_pri_rate*
Cbd	0.9938	25.84%	6.2031	18.75%
Others	0.9402	28.59%	4.6776	25.68%
Overall	0.9583	27.88%	5.0729	23.89%

*Region: The type of area; P_average: The average electricity price; Occ_rate: The occupancy rate; N_neig: The number of neighboring regions. Dyn_pri_rate: The dynamic pricing rate in this area.

As shown in the Figure 2, the input data includes detailed information on 247 transportation zones with EV charging data, with 23.89% of the zones using a time-of-use (TOU) pricing scheme and the remaining zones using a fixed pricing scheme. The Central Business District (CBD) consists of 62 transportation zones. This experiment applies working days from 30 days of data (21 days in total), sampled every ten

minutes, for a total of 3024 timestamps ($6 \times 24 \times 21$). Containing all 21 days of tariffs, occupancy rate, description of the CBD and dynamic tariff situation of the site, neighboring region information, etc., the maximum tariff difference between the region and neighboring regions is calculated. Experiments are conducted with real data to ensure the authenticity of the results and make them practical for engineering and academic purposes.

B. Clustering results

The clustering method and the number of clusters require to be judged by the root mean square error after regression through the decision tree. In the process, we compared various regression methods. It was found that decision tree regression was effective in capturing the overall trend between electricity prices and occupancy rates. Compared to linear regression and support vector regression (SVR), decision tree regression typically provides a more stable and accurate fit.

In terms of clustering methods, we tried 9 methods: Aggregation, GMM and K-Means, separate sum, cosine, Manhattan, and Euclidean combination. By comparing their Root Mean Square Error (RMSE), in Figure 3, K-means-Cosine-4 was chosen as the clustering method.

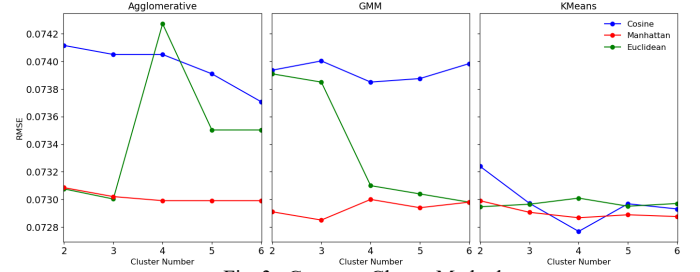


Fig. 3. Compare Cluster Methods

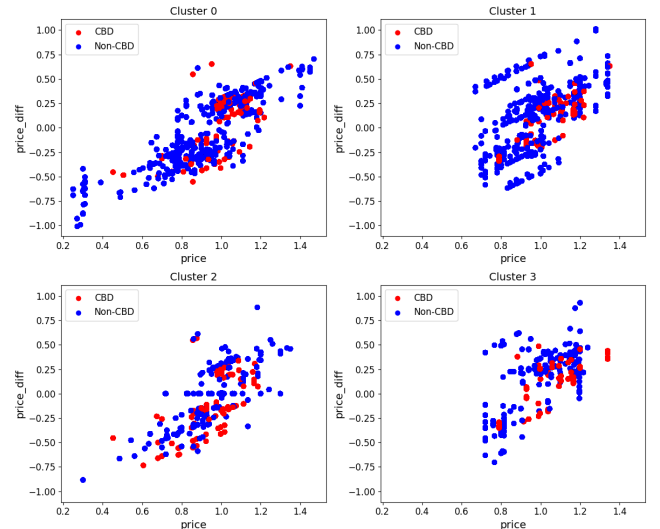


Fig. 4. Cluster Results

The clustering result is shown in Figure 4, with the red points representing the CBD area and the blue ones representing the other areas. The results obtained from the fitting are shown in Figure 5. The blue color is the actual occupancy rate, and the red color is the occupancy rate obtained from the regression. It can be seen that in the regression results, the trends are basically the same.

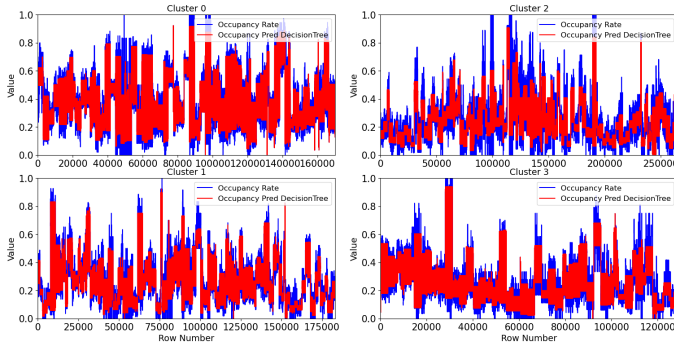


Fig. 5. Clustered Data Regression

TABLE II. REPRESENTATIVE DATA FOR CLUSTERS

Region	Price	P_diff	Occ_rate	Dyn_pri_rate	CBD_rate
All	0.9583	0.0307	27.88%	23.89%	25.91%
Cluster0	0.8754	-0.1283	36.84%	84.33%	22.36%
Cluster1	0.9904	0.1385	26.43%	9.75%	19.41%
Cluster2	0.9682	-0.0011	24.14%	2.99%	31.12%
Cluster3	0.9979	0.1531	25.78%	7.17%	29.12%

Table 2 lists five key metrics used to assess inter-cluster differences: Price, P_diff, Occ_rate(occupancy_rate), Dyn_pri_rate(dynamic pricing rate in this area), and CBD_rate, where P_diff is defined as the difference between local area tariffs and neighboring area tariffs ($P_diff = \text{local tariff} - \text{neighboring tariff}$). A positive value means that the local tariff is lower than the neighboring tariff, and a negative value means that the local tariff is higher than the neighboring tariff.

- Cluster 0: In cluster 0, P_diff is negative, which clearly indicates that the local tariff is lower than the neighboring tariffs. This cluster also has the highest utilization rate (36.84%), which indicates that the lower local price contributes to higher utilization rate.
- Cluster 1: In cluster 1, a positive P_diff indicates that local electricity prices are higher than in neighboring areas. This corresponds to a medium level of occupancy (26.43%).
- Cluster 2: the P_diff for cluster 2 is almost zero, indicating that the local price is almost the same as the neighboring areas.
- Cluster 3: Cluster 3 has the highest absolute price with a positive P_diff, higher local price than the neighboring region's price, and a moderate occupancy rate (25.78%).

The results show that when local prices are significantly lower than in neighboring areas, occupancy rates increase significantly. When local prices are significantly higher than in neighboring areas, occupancy rates decrease significantly.

C. User Behavioral Analysis

In the analysis in this chapter, we choose the CBD (Central Business District) area as the analysis object of the typical case. It mainly based on the following reasons: First, CBD areas usually have a stable electricity demand, which can reflect the impact of tariff strategies on occupancy rates more clearly; Secondly, the tariff and occupancy data in CBD areas are driven by business activities, which are more regular and representative,

it can effectively exclude possible disturbances introduced by other areas such as residential or industrial areas.

We delve into the impact of tariff strategies on occupancy rate by analyzing the typical characteristics of four clusters. Each cluster exhibits significant differences in tariff spread (P_diff), Occupancy Rate, and the relationship between occupancy rate and tariff. In order to understand these differences more comprehensively, we conduct a detailed analysis of each cluster in conjunction with the data features in the graphs, and further explore the reasons behind and potential optimization strategies. The following are the specific analyses of the four clusters.

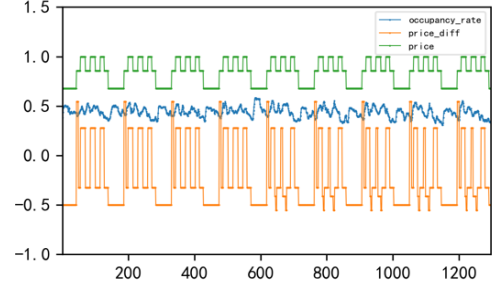


Fig. 6. Clustered 0 Example

In Cluster 0, the main feature presents the local electricity price is significantly lower than the neighboring regions, which directly leads to a higher occupancy rate. Most of the tariffs in this category apply a dynamic tariff strategy with small fluctuations. This strategy is particularly effective in the CBD area, attracting more users and increasing the overall occupancy rate while optimizing the matching of supply and demand through dynamic tariff regulation.

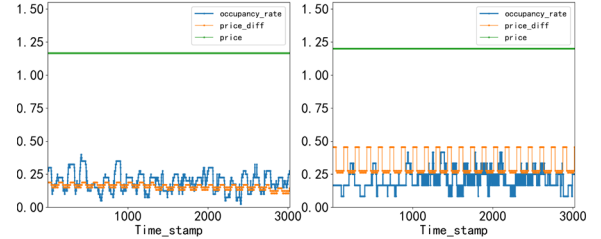


Fig. 7. Clustered 1 and 3 Example

In this case, through the analysis of Cluster 1 and Cluster 3, it is found that the occupancy rate is consistently maintained at a lower level when the local electricity price is higher than the neighboring regions for a long period of time. The data in Figure 7 shows that P_diff is always positive, indicating that the local electricity price is significantly higher than the neighboring electricity price. In this case, the occupancy rate shows a certain response to the fluctuation of the neighboring electricity price: when the neighboring electricity price rises, the relative advantage of the local region's electricity price increases, and the occupancy rate then appears to rise to a certain extent. On the contrary, when the neighboring electricity price decreases, the relative disadvantage of the local region's electricity price is intensified, and the occupancy rate further decreases. However, although the occupancy rate varies with fluctuations in neighboring tariffs, its overall level remains consistently in the lower range.

This phenomenon suggests that when electricity prices in the region are chronically higher than those in neighboring regions, users are more inclined to choose a neighboring region with lower electricity prices, thus making it difficult for the occupancy rate in the region to increase significantly. Regardless of the degree of fluctuation of neighboring tariffs, the inhibitory effect of the fixed-high tariff strategy on the occupancy rate always exists, which ultimately keeps the occupancy rate at a low level.

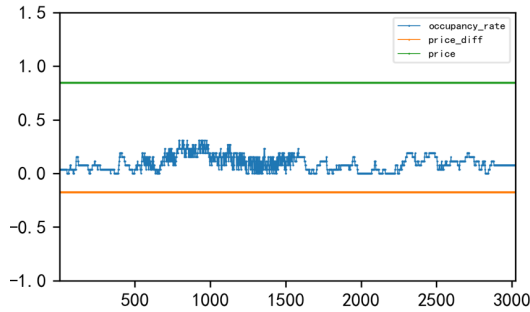


Fig. 8. Clustered 2 Example

From the data in Cluster 2, it can be observed that the occupancy curve fluctuates within a small range and the occupancy level is low when both local tariffs and neighboring tariffs are fixed.

D. Discussion

The results of this study show the important impact of tariff strategies on occupancy rates. Dynamic pricing strategies (e.g., Cluster 0) effectively increase occupancy when local tariffs are lower than neighboring areas. In contrast, fixed high tariff strategies (e.g., Cluster 1 and 3) tend to discourage occupancy, even when neighborhood tariffs fluctuate. Notably, Cluster 2, where local tariffs are almost equal to neighboring tariffs, has the lowest occupancy rates, suggesting that tariff parity alone is not sufficient to attract users. These insights are in line with previous studies on the interaction between pricing strategies and user behavior in urban energy systems [15,16,177]. Future research could explore the incorporation of non-tariff factors, such as regional competitiveness, into pricing models to further optimize regional occupancy and improve the effectiveness of tariff strategies.

IV. CONCLUSIONS

This paper develops a data-driven methodology to analyze the impact of tariff strategies on electric vehicle (EV) charging behavior, with a focus on the relationship between local and neighboring tariffs and occupancy rates. By leveraging a dataset from Shenzhen, China, and employing techniques such as LSTM-based dimensionality reduction, cosine similarity-based K-means clustering, and decision tree regression, identifies four distinct clusters of charging stations based on pricing patterns and user behavior.

The results of the study show that dynamic pricing strategies significantly increase occupancy when local tariffs are lower than those of neighboring regions. In contrast, fixed high tariff strategies tend to discourage occupancy, even when neighboring tariffs fluctuate. Fixed local and neighboring tariffs and a

slightly lower local tariff than neighboring tariffs have the lowest occupancy rate, suggesting that tariff parity alone is not sufficient to attract users. These findings provide valuable insights into optimizing pricing strategies for urban EV charging infrastructure, highlighting the importance of incorporating non-tariff factors such as regional competitiveness into future models. The proposed methodology is practical, scalable and industry-friendly, providing a flexible framework for improving the efficiency and sustainability of EV charging networks.

REFERENCES

- [1] Gartner, "Gartner: Global Electric Vehicle Fleet Will Reach 85 Million by End of 2025," Gartner Press Release, Beijing, November 21, 2024. [Online]. Available: <https://www.gartner.com/cn/newsroom/press-releases/2024-ev-forecast>.
- [2] S. Borlaug, M. Muratori, and T. E. Lipman, "Public charging infrastructure utilization patterns in the United States," *Energy Policy*, vol. 181, Art. no. 113722, 2023.
- [3] J. Kim, H. Moon, and S. Park, "Subsidy-driven distortions in South Korean EV charging markets," *Energy Econ.*, vol. 115, Art. no. 106373, 2022.
- [4] Z. Zhao and C. K. M. Lee, "Dynamic pricing for EV charging stations: A deep reinforcement learning approach," *IEEE Trans. Transp. Electrification*, vol. 8, no. 2, pp. 2456–2468, 2022.
- [5] B. Palaniyappan, R. Senthil Kumar, and T. Vinopraha, "Dynamic pricing for load shifting: Reducing electric vehicle charging impacts on the grid through machine learning-based demand response," *Sustain. Cities Soc.*, vol. 103, Art. no. 105256, 2024.
- [6] M. Skare, D. R. Soriano, and M. Porada-Rochon, "Impact of COVID-19 on the travel and tourism industry," *Technol. Forecast. Soc. Change*, vol. 163, Art. no. 120469, 2021.
- [7] N. Rivers and B. Schaufele, "Carbon tax salience: Experimental evidence from British Columbia," *Energy Econ.*, vol. 65, pp. 1–8, 2017.
- [8] J. H. Lee, D. Chakraborty, S. J. Hardman, and G. Tal, "Exploring electric vehicle charging patterns: Mixed usage of charging infrastructure," *Transp. Res. Part D: Transp. Environ.*, vol. 79, Art. no. 102249, 2020.
- [9] I. Ullah, K. Liu, T. Yamamoto, M. Zahid, and A. Jamal, "Modeling of machine learning with SHAP approach for electric vehicle charging station choice behavior prediction," *Travel Behav. Soc.*, vol. 31, pp. 78–92, 2023.
- [10] I. Ullah, K. Liu, T. Yamamoto, M. Zahid, and A. Jamal, "Modeling of machine learning with SHAP approach for electric vehicle charging station choice behavior prediction," *Travel Behav. Soc.*, vol. 31, pp. 78–92, 2023.
- [11] A. Almutairi and T. M. Aljohani, "Reliability-driven time-of-use tariffs for efficient plug-in electric vehicle integration," *Sustain. Cities Soc.*, vol. 107, Art. no. 105463, 2024, doi:10.1016/j.scs.2024.105463.
- [12] L. Jian, Y. Zheng, and X. Luo, "Time-of-use tariff design for EV charging stations: A Shanghai case study," *IEEE Trans. Smart Grid*, vol. 9, no. 4, pp. 3252–3260, 2018.
- [13] P. Martins, F. Moura, and J. de Almeida, "EU policy impacts on electric vehicle adoption: A multicountry analysis," *Transp. Res. Part D: Transp. Environ.*, vol. 122, Art. no. 103885, 2023, doi:10.1016/j.trd.2023.103885.
- [14] Intelligent Systems Lab, "Spatio-temporal EVCDP (Shenzhen)" [Data set]. GitHub. Available: <https://github.com/IntelligentSystemsLab/ST-EVCDP>
- [15] J. Smith and L. Johnson, "The impact of aerofoil thickness on wind turbine blade performance," *Renewable Energy Journal*, vol. 45, no. 3, pp. 123–135, 2020.
- [16] R. Brown and K. Davis, "Shape variations and their effects on wind turbine efficiency," *Journal of Fluid Dynamics*, vol. 58, no. 2, pp. 234–248, 2021.
- [17] M. Lee and P. Taylor, "Fluid-structure bend-twist coupling in wind turbine blades: A comprehensive analysis," *Energy Systems Research*, vol. 12, no. 4, pp. 567–580, 2022.